Proceedings of ISFOG 2025
5TH INTERNATIONAL SYMPOSIUM ON
FRONTIERS IN OFFSHORE GEOTECHNICS
Nantes, France | June 9-13 2025

ISBN 978-2-85782-758-0

Undrained capacity of suction buckets under VHM loads in cohesive soil

X. Feng*, and Q. Zhao
Dalian University of Technology, Dalian, China
**xfeng@dlut.edu.cn (corresponding author)*

ABSTRACT: Suction buckets are commonly used as support foundations for offshore fixed structures. A procedure of determining the VHM failure envelopes of the suction buckets is proposed. Firstly, the soil failure mechanisms around the suction buckets in absence of the vertical load are studied by finite element analyses. Based on the failure mechanisms obtained, analytical solutions for calculating the HM capacity are established. All the governing parameters of the elliptical failure envelope in the HM plane are demonstrated to have a physical meaning. The HM failure envelopes are found to contract as the vertical load V increases. For a given vertical load, the HM failure envelope can be determined by scaling down the semi-major and semi-minor axes with the oblique angle of major axis unchanged. The scaling factors can be respectively derived from the V-H and V-M interaction diagrams. The results show that the closed form expressions, with all relevant parameters being physically sensible, are consistent with the results of detailed 3D finite element analyses for the considered boundary conditions.

Keywords: Suction; skirted foundations; bearing capacity; offshore engineering

1 INTRODUCTION

Suction buckets are circular skirted foundations akin to the inverted buckets, which are widely applied in offshore resource developments. Suction bucket foundations have been used as anchor foundations for offshore floating facilities since 1980s. When used for catenary or taut mooring, the main task of the design is to analyse the optimal position of the padeye and the load-carrying capacity of the anchor foundation under inclined loads induced by the chain tension at the padeye (Kennedy et al., 2013). Suction bucket foundations are also commonly used as support foundations of offshore fixed structures, such as subsea production facilities (Kay and Palix, 2011), and jacket structures for offshore wind turbines (Sturm, 2019). Unlike suction anchors, support foundations are typically subjected to a combination of significant vertical loads V, horizontal loads H and moment loads M during service, which are applied to the top cap rather than at a padeye below the seafloor. The embedded length to diameter ratios L/D of the suction buckets used as support foundations are typically smaller, about 1-3, compared to anchor foundations which usually have L/D=3-6. Therefore, when the suction buckets are used as support foundations, the design considerations of assessing the load-carrying capacity are different from that of the suction anchors.

This paper will study the undrained capacity of the suction buckets used as support foundations subject to VHM loading. Intially, equations describing the HM failure envelopes are briefly introduced. Finite element (FE) modelling is subsequently carried out in order to establish the analytical solutions for calculating all the governing parameters. An approach is finally proposed to derive the complete VHM failure envelopes of the suction buckets.

2 DEFINITION OF THE HM FAILURE ENVELOPES

The undrained capacity of the circular skirted foundations under combined VHM loading can be presented in form of the failure envelopes in the HM plane, which are typically a family of contracting ellipse with increasing V, e.g. (Vulpe et al., 2014, Gerolymos et al., 2015, Biswas and Choudhury, 2023).The undrained ultimate capacity of the bucket foundations with L/D=0.5~6 was investigated in homogeneous, normally consolidated and layered soils (Palix et al., 2010, Kay and Palix, 2010, Kay, 2015). A rotated ellipse is proposed to describe the failure envelopes

$$\left(\frac{H^{*}cos\psi_{MH}-M^{*}sin\psi_{MH}}{a_{MH}}\right)^{2}+\left(\frac{H^{*}sin\psi_{MH}+M^{*}cos\psi_{MH}}{b_{MH}}\right)^{2}=1 \quad (1)$$

where $H^{*}=H/(DLs_{u,avg})$ and $M^{*}=M/(DL^{2}s_{u,avg})$ are respectively the dimensionless horizontal and moment capacity, and $s_{u,avg}$ is the average undrained shear strength within the embedment depth. As shown in Figure 1, the semi-major axis a_{MH} can be determined by the maximum horizontal capacity H_{max} and the oblique angle of the major axis ψ_{MH}, i.e.

$$a_{MH} = \frac{H_{max}}{DLs_{u,avg}cos\psi_{MH}} \quad (2)$$

The oblique angle ψ_{MH} (clockwise rotation taken as positive) is considered to be related to the centroid of the profile of undrained shear strength with depth $e_{z,su}$ (Kay and Palix, 2010)

$$\psi_{MH} = tan^{-1}\frac{e_{z,su}}{L} + \Delta\psi_{MH} \quad (3)$$

The semi-minor axis b_{MH} is calculated from the pure horizontal capacity H_{ult} by

$$b_{MH} = \frac{H_{ult}}{DLs_{u,avg}}sin\psi_{MH} + \Delta b_{MH} \quad (4)$$

In Eq. (3) it is sensible to correlate ψ_{MH} with $e_{z,su}$. However, it is found that the value of ψ_{MH} is relevant not only to the soil undrained shear strength profile, but also to the embedment depth ratio. In addition, the semi-minor axis OB as shown in Figure 1 is not necessarily orthogonal to BC. As a result, the correction terms $\Delta\psi_{MH}$ and Δb_{MH} are included in Eqs. (3) and (4), respectively, to define the oblique angle and the semi-minor axis. Therefore, although the parameters given in Eqs. (2) to (4) are somewhat physically sensible, they still cannot be strictly defined. Corrections need to be made by curve-fitting from results of extensive numerical analyses, hindering convenient application in the engineering design.

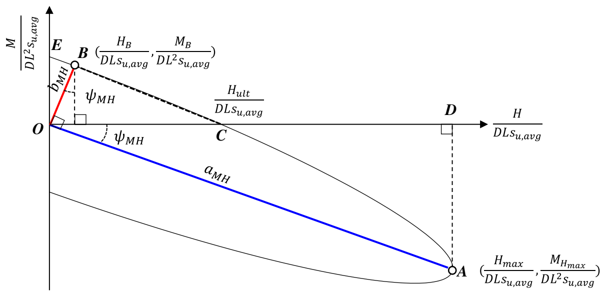

Figure 1. The elliptic function and the governing parameters of the HM failure envelopes

3 PROBLEM DEFINITION AND FINITE ELEMENT MODELLING

A suction bucket with a diameter of D and an embedded length L was considered. The wall thickness was set as t =1%D. The soil undrained shear strength increased proportionally with depth z according to $s_u = s_{um} + kz$, where s_{um} is the undrained shear strength at mudline and k is the gradient of undrained shear strength with depth. The heterogeneity factor of the undrained shear strength is defined as $\kappa = kD/s_{um}$. The problem definition is shown in Figure 2.

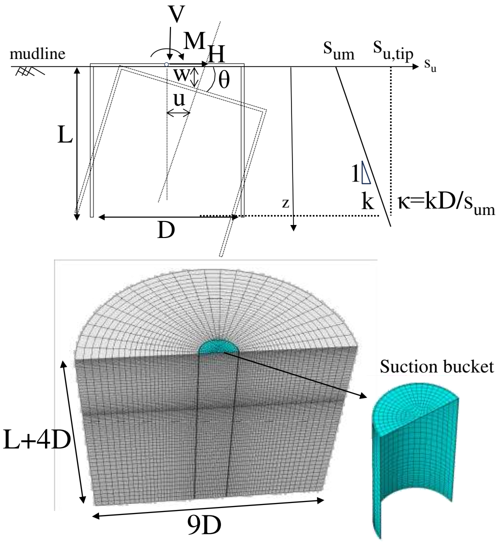

Figure 2. Problem definition and example FE mesh (L/D=2.0)

The FE analyses were carried out using the software package ABAQUS 6.14 (Dassault Systèmes, 2014). The diameter of suction buckets remained constant as D=10m, while the embedded length varied with the predefined embedment depth ratios L/D=1, 2 and 3. Since the HM loads are co-planar only half of the model was analysed considering the model symmetry. The side boundary of the mesh extended outwards by 4D from the centerline of the bucket, and the bottom boundary extended downwards by 4D from the tip. The side nodes were radially constrained, while the bottom nodes were fixed at all directions. A region of very thin elements (~1%D) was employed around the external and internal side of the bucket with the local soil strength (i.e. friction) taken as 0.65s_u. The soil domain was discretised using the C3D8H elements. An example mesh is shown in Figure 2. The soil was modelled as linear elastic, perfectly plastic obeying a Tresca failure criterion. The elastic properties were defined by undrained Young's modulus E_u = 500s_u and Poisson's ratio of v = 0.49. The bucket was constrained as a rigid body, with the motion controlled by a reference node at the centre of caisson at mudline. No detachment is permitted for the bucket-soil interface. Fix-displacement-ratio probe tests were used to detect the failure envelopes.

4 RESULTS

4.1 Example HM failure envelope and typical soil failure mechanisms

An example HM failure envelope for L/D = 2.0 and κ = 0 is shown in Figure 3, together with the FE result of the soil displacement contours of each representative point on the envelope. According to Randolph and House (2002), when the bucket foundation rotated forward the soil failure mechanism consisted of a conical wedge mechanism, a flow-around mechanism and an extended spherical shearing surface around the bucket (Figure 4a). When the bucket foundation translated transversally, the maximum horizontal capacity was mobilised where the extended spherical failure surface in Figure 4a transformed to a shear failure along the foundation base (Figure 4b). For small *L/D* ratio, the wedge mechanism immediately connected to the extended spherical surface with the flow-around mechanism vanished.

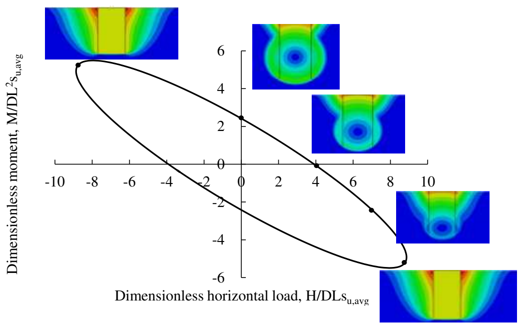

Figure 3.FE results of HM failure envelop and typical soil failure mechanisms of representing loading paths

For a foundation rotating forwards the horizontal and moment capacity can be calculated by Eq. (5) based on the failure mechanism shown in Figure 4a.

$$(H \cdot z_c + M)\omega = \dot{D}_h + \dot{D}_b \tag{5}$$

where $\dot{D}_h$ is the rate of work dissipation due to the side resistance

$$\dot{D}_h = \int_0^{2z_c - L} N_p D s_u (z_c - z)\omega dz \tag{6}$$

and $\dot{D}_b$ is the rate of work dissipation along the spherical shearing surface

$$\dot{D}_b = \int_0^{2\pi}\int_0^{\psi_2} \omega s_u R_2^3 \cdot \sqrt{(sin\psi sin\varphi)^2 + (cos\psi)^2} sin\psi d\psi d\varphi \tag{7}$$

with

$$R_2 = \sqrt{(L - z_c)^2 + R^2}$$
$$\psi_2 = \pi - tan^{-1}\frac{R}{L - z_c} \tag{8}$$

where z_c is centre of rotation and N_p is the dimensionless lateral bearing factor.

For a translating foundation shown in Figure 4b the maximum horizontal capacity was mobilised and can be calculated from

$$H_{max} = \frac{\pi}{4}D^2 s_{u,tip} + \int_0^L N_p D s_u dz \tag{9}$$

where $s_{u,tip}$ is the local soil shear strength at the foundation tip.

As can be seen from Eqs. (6) and (9), the key issue is to determine the profile of the dimensionless lateral bearing factor N_p before solving the ultimate capacity corresponding to the two typical failure modes, which will be presented separately in the next section.

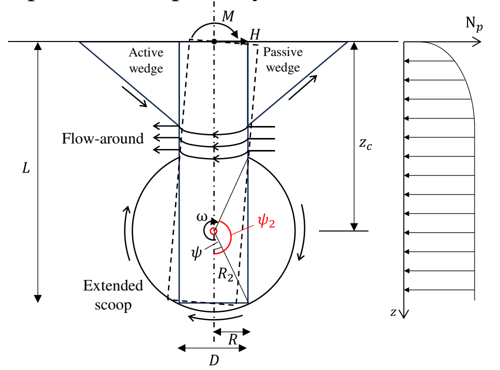

(a) Buckets with forward rotation

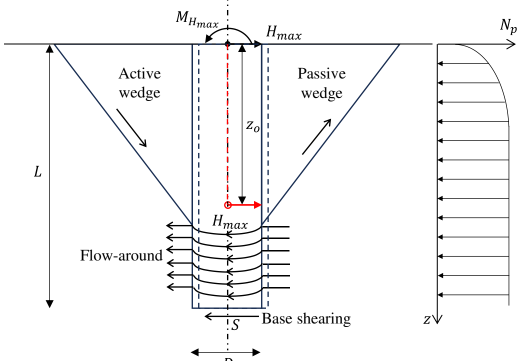

(b) Buckets with lateral translation

Figure 4. Analytical model for calculating the capacity of a forward rotating and a translating suction bucket

4.2 Profile of dimensionless lateral bearing factor N_p

The dimensionless lateral bearing capacity factor N_p with depth *z* was determined from the finite element analyses following Grajales-Saavedra et al. (2017). The lateral bearing factor N_p for the one-sided mechanism in the weightless soils was obtained from the FE analyses and can be fitted by the empirical expression proposed by (Murff and Hamilton, 1993)

$$N_p = N_1 - (N_1 - N_2) \cdot \exp(-\xi \frac{z}{D}) \qquad (10)$$

where $N_1 = 9.14+4.14\alpha-1.34\alpha^2$ (Martin and Randolph, 2006), and $N_2 = 2+1.22\alpha$, with α being the shaft friction ratio. The parameter ξ is only a function of κ and reflects the rate of increase of N_p from the mudline value N_2 to its limiting value N_1, where the shallow conical wedge mechanism gradually transformed to the flow-around mechanism.

$$\xi = \begin{cases} 0.22 + 0.02\lambda & \lambda \leq 10 \\ 0.42 & \lambda > 10 \end{cases} \qquad (11)$$

with $\lambda = 1/\kappa$.

If full adhesion is assumed for the active wedge on the trailing side of the bucket, the computed value of N_p in Eq. (10) should be doubled, subject to the restriction that N_p does not exceed the limited value N_1.

4.3 Solving HM failure envelope parameters

4.3.1 Semi-major axis a_{MH} and the oblique angle ψ_{MH}

The maximum horizontal capacity H_{max} of a translating bucket had been determined by Eq. (9), while the oblique angle of the major axis ψ_{MH} can be derived from Figure 1 by

$$\psi_{MH} = tan^{-1}\frac{M_{H_{max}}}{H_{max} \cdot L} = tan^{-1}\frac{z_o}{L} \qquad (12)$$

where, M_{Hmax} is the moment required to resist the rotation when the horizontal load H_{max} is applied to the top cap, which results in a pure translation of the bucket. According to the force translation theorem, $M_{H_{max}} = H_{max} \cdot z_o$ with z_o being the depth at which only when an equivalent single horizontal load H_{max} acted along the central axis causing translational failure. The value of z_o can be solved from

$$S(L - z_o) + \int_0^L N_p s_u D(z - z_o)dz = 0 \qquad (13)$$

where S is the base shear. Thereafter, the semi-major axis a_{MH} can be computed by Eq. (2).

4.3.2 Semi-minor axis b_{MH}

The semi-minor axis b_{MH} can be obtained from the capacity of point B in Figure 1, i.e. the intersection of the semi-minor axis with the failure envelope. At point B the horizontal load and the moment satisfied

$$\frac{H}{M} = \frac{tan\psi_{MH}}{L} = \frac{z_o}{L^2} \qquad (14)$$

The failure mechanism of point B conformed to that shown in Figure 4a. Combine Eq. (14) with Eq. (5) to (8), the moment capacity at point B can be solved. Since $\dot{D}_h$ and $\dot{D}_b$ are related to the centre of rotation z_c, the moment capacity at point B can be determined as the minimum value of M with respect to z_c. Then, b_{MH} can be calculated by

$$b_{MH} = \sqrt{\left(\frac{H}{DLs_{u,avg}}\right)^2 + \left(\frac{M}{DL^2 s_{u,avg}}\right)^2} \qquad (15)$$

4.3.3 Comparison with the FE results

The computed values of a_{MH}, ψ_{MH} and b_{MH} from the preceding sections were substituted into Eq. (1), and the derived failure envelopes were compared with the FE results. Figure 5a to c respectively shows the variations in the size and shape of the HM failure envelope with increasing κ for L/D = 1.0, 2.0 and 3.0. Except for low κ ≤ 1, the analytical solutions of the HM failure envelopes fall slightly inside the FE results, i.e. more conservative for all the considered L/D.

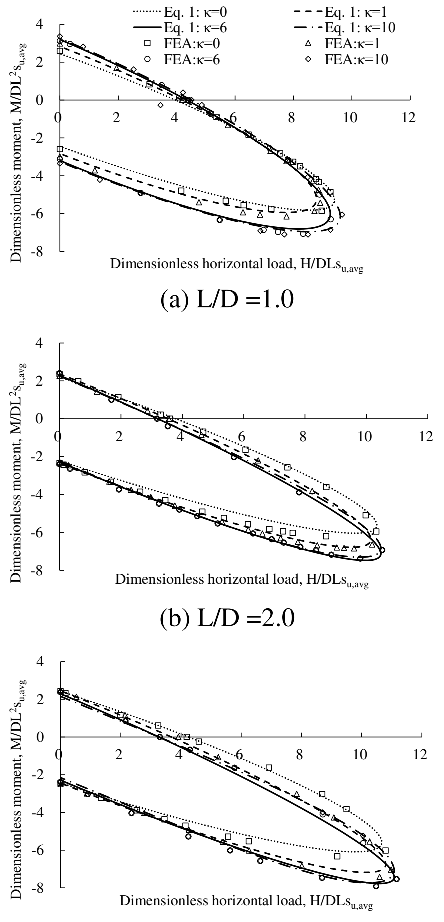

(a) L/D =1.0

(b) L/D =2.0

(c) L/D =3.0

Figure 5. Comparisons of the derived HM failure envelopes with FE results

4.4 Effect of the vertical load on the HM failure envelopes

The effect of the vertical force *V* on the *HM* failure envelope is presented in Figure 6. As the magnitude of the vertical load increases, the failure envelopes contract inwards where the semi-major and semi-minor axis reduces. However, the oblique angle of the major axis was not affected. Since the semi-major axis is calculated from the horizontal capacity associated with the translational failure of the bucket foundations, the semi-major axis of a given *V* can be computed using the *VH* failure envelopes of a translating bucket, which can be described by Eq. (16) (Supachawarote et al., 2004)

$$\left(\frac{H}{H_{max}}\right)^{0.5+\frac{L}{D}}+\left(\frac{V}{V_{ult}}\right)^{4.5-\frac{L}{3D}}=1 \qquad (16)$$

The semi-minor axis was determined by the capacity of a forward rotating bucket under combined HM loading. The point E on the failure envelope in Figure 1 corresponds to the capacity of a rotating bucket subject to a pure moment load. Figure 6 shows that as the vertical load increases the length of OE and OB in Figure 1 reduces in approximately the same proportion. Therefore, the semi-minor axis for a given V can be obtained by the V-M failure envelopes which might be described by

$$\left(\frac{M}{M_{ult}}\right)^{0.7+\frac{L}{D}}+\left(\frac{V}{V_{ult}}\right)^{2.5-\frac{L}{10D}}=1 \qquad (17)$$

The effect of the vertical load *V* on the *HM* failure envelopes can be evaluated following the procedure in Kay and Palix (2010). With the oblique angle remain constant, the semi-major and semi-minor axes of the HM ellipse for non-zero vertical load can be derived by scaling down those at V=0 using a factor of H/H_{max} by Eq. (16) and M/M_{ult} by Eq. (17), respectively. Figure 6 gives an example case of various L/D ratios at κ=10, demonstrating the good agreement between the calculated VHM failure envelopes and FE results.

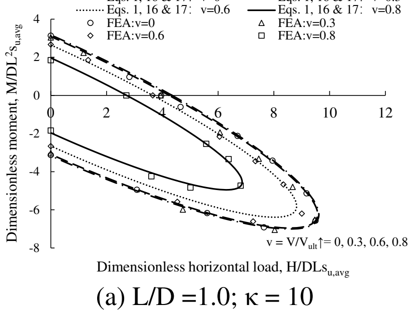

(a) L/D =1.0; κ = 10

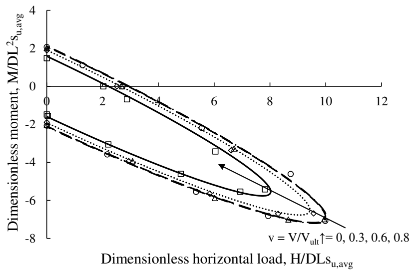

(b) L/D =2.0; κ = 10

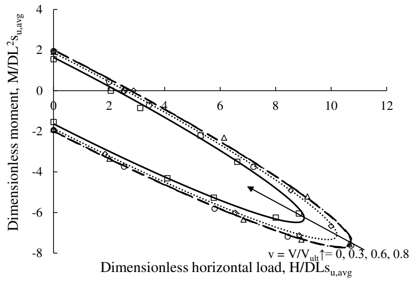

(c) L/D =3.0; κ = 10

Figure 6. Comparisons of the complete VHM failure envelopes with FE results

5 CONCLUSIONS

This study investigates the undrained VHM capacity of suction buckets used as support foundations embedded in cohesive soil with L/D=1 to 3. In absence of the vertical load the HM resistance of the suction buckets can be described by a rotated ellipse in the dimensionless HM plane. The parameters governing the shape and size of the failure envelopes, including the semi-major axis, the oblique angle of the major axis and the semi-minor axis, have been calculated and proven to be physically sensible. The results show that the closed form expressions agree well with the FE results. An approach is then established to derive the complete VHM failure envelopes of the suction buckets. Therefore, the procedure can be adopted in engineering practice for efficient assessment of the governing load cases and optimisation of suction buckets.

AUTHOR CONTRIBUTION STATEMENT

Xiaowei Feng:, Conceptualization, Methodology, Supervision, Writing- Reviewing and Editing. **Qian Zhao**: Writing- Original draft, Formal Analysis.

ACKNOWLEDGEMENTS

The authors are grateful for the support provided by the National Natural Science Foundation of China (no.52271262).

REFERENCES

Biswas, S. and Choudhury, D. (2023) Design Approach for Deeply Embedded Circular Caisson Foundations under Combined Loading. *Int J Geomech* **23(7)**:04023091.

Dassault Systèmes (2014) *ABAQUS 6.14 Analysis User's Manual.* Simulia Corp, Providence, RI, USA.

Gerolymos, N., Zafeirakos, A. and Karapiperis, K. (2015) Generalized failure envelope for caisson foundations in cohesive soil: Static and dynamic loading. *Soil Dynamics and Earthquake Engineering* **78**:154-174.

Grajales-Saavedra, F. J., Aubeny, C. P., Jeanjean, P. and Drew, D. (2017) Plastic Limit Analysis of Laterally Loaded Piles and Wells Conductors in Soil Profiles with Crust. *Proc. of Offshore Technology Conference*, Houston, Texas, USA, OTC-27785-MS. OTC.

Kay, S. (2015) CAISSON_VHM: A program for caisson capacity under VHM load in undrained soils. *Proc. of 3rd International Symposium on Frontiers in Offshore Geotechnics (ISFOG 2015)*, Oslo, Norway, V. Meyer (eds.), pp. 277-282. CRC Press/Balkema.

Kay, S. and Palix, E. (2010) Caisson capacity in clay: VHM resistance envelope – Part 2: VHM envelope equation and design procedures. *Proc. of 2nd Internation Symposium on Frontiers in Offshore Geotechniques (ISFOG 2010)*, Perth, Western Austrailia, S. Gourvenec & D. White (eds.), pp. 741-746.

Kay, S. and Palix, E. (2011) Caisson capacity in clay: VHM resistance envelope: Part 3—extension to shallow foundations. *Proc. of ASME 2011 30th International Conference on Ocean, Offshore and Arctic Engineering*, (eds.) vol. Volume 7: CFD and VIV; Offshore Geotechnics, pp. 789-798.

Kennedy, J., Oliphant, J., Maconochie, A., Stuyts, B. and Cathie, D. (2013) CAISSON: A suction pile design tool. *Proc. of 32nd International Conference on Ocean, Offshore and Arctic Engineering (OMAE 2013)*, Nantes, France, vol. Volume 6: Polar and Arctic Sciences and Technology; Offshore Geotechnics; Petroleum Technology Symposium, V006T10A030. ASME.

Martin, C. M. and Randolph, M. F. (2006) Upper-bound analysis of lateral pile capacity in cohesive soil. *Géotechnique* **56(2)**:141-145.

Murff, J. D. and Hamilton, J. M. (1993) P-ultimate for undrained analysis of laterally loaded piles. *J Geotech Eng ASCE* **119(1)**:91-107.

Palix, E., Willems, T. and Kay, S. (2010) Caisson capacity in clay: VHM resistance envelope – Part1: 3D FEM numerical study. *Proc. of 2nd Internation Symposium on Frontiers in Offshore Geotechniques (ISFOG 2010)*, Perth, Western Australlia, S. Gourvenec & D. White (eds.), pp. 753-758.

Randolph, M. and House, A. (2002) Analysis of suction caisson capacity in clay. *Proc. of Offshore Technology Conference*, Houston, Texas, OTC-14236-MS. Offshore Technology Conference.

Sturm, H. (2019) Design aspects of suction caissons for offshore wind turbine foundations. *Proc. of TC209 Workshop on Foundation Design of Offshore Wind Structures*, Seoul, Y. Shin (eds.), pp. 45-63. ISSMGE.

Supachawarote, C., Randolph, M. and Gourvenec, S. (2004) Inclined pull-out capacity of suction caissons. *Proc. of the 14th International Offshore and Polar Engineering Conference*, Toulon, France, (eds.), pp. 500-506. ISOPE.

Vulpe, C., Gourvenec, S. and Power, M. (2014) A generalised failure envelope for undrained capacity of circular shallow foundations under general loading. *Géotechnique Letters* **4(3)**:187-196.